# Synchrotron x-ray-scattering study of the normal-incommensurate phase transition in $Rb_2ZnCl_4$

M. P. Zinkin
*Oxford Physics, Clarendon Laboratory, Parks Road, Oxford OX1 3PU, United Kingdom*

D. F. McMorrow
*Department of Solid State Physics, Risø National Laboratory, DK-4000 Roskilde, Denmark*

J. P. Hill
*Department of Physics, Brookhaven National Laboratory, Upton, New York 11973*

R. A. Cowley
*Oxford Physics, Clarendon Laboratory, Parks Road, Oxford OX1 3PU, United Kingdom*

J.-G. Lussier
*Department of Solid State Physics, Risø National Laboratory, DK-4000 Roskilde, Denmark*

A. Gibaud
*Université du Maine, Faculté des Sciences, URA No. 807 CNRS, Avenue Olivier Messian, 72017 Le Mans Cedex, France*

G. Grübel and C. Sutter
*European Synchrotron Radiation Facility, Boîte Postale 220, 38043 Grenoble Cedex, France*

(Received 18 January 1996)

The results of high-resolution synchrotron x-ray-scattering experiments on the normal-incommensurate phase transition in $Rb_2ZnCl_4$ are reported. Measured critical exponents for the intensities of the first three harmonics of the incommensurate modulation wave below $T_c$ agree well with theoretical predictions for the $n=2$, $D=3$ (3D-$XY$) universality class. The scattering observed above $T_c$ corrresponds to critical fluctuations on two distinct length scales: the critical exponents for the short length scale component of the scattering agree with those expected for the 3D-$XY$ universality class. The value found for the exponent of the inverse correlation length of the long length scale component is $\nu_s=0.7\pm0.2$. A comparison of data taken in Laue and Bragg geometries at different photon energies suggests that the second length scale scattering originates in the near-surface region. Possible explanations of the two length scale behavior are discussed. [S0163-1829(96)04225-7]

## I. INTRODUCTION

This paper reports a detailed study of the normal-incommensurate structural phase transition of $Rb_2ZnCl_4$ using synchrotron x-ray-scattering techniques. The development of synchrotron sources allows x-ray-scattering measurements to be performed with higher intensities and better wave-vector resolution than was possible previously, and these improvements should permit a quantitative study of the ordering and fluctuations associated with structural phase transitions, at temperatures both very close to, and far from the transition temperature. Of particular interest in this paper are the data on two topical questions: first, on the critical exponents of the order parameters and critical scattering at higher harmonics of the ordering wave vector, and second, on whether this class of phase transitions exhibits the two length scale behavior found in x-ray and neutron-scattering studies of other structural and magnetic phase transitions. The results show that the scattering associated with the higher harmonics is consistent with the prediction of renormalization-group theories, and that close to but above $T_c$, two length scale behavior is observed in this system.

$Rb_2ZnCl_4$ was chosen for investigation because it has a well-studied continuous phase transition from a high-temperature normal phase with the $\beta$-$K_2SO_4$ structure (space group $Pmcn$), to a low-temperature one-dimensionally modulated incommensurate phase characterized by a modulation wave vector **q.** The modulation arises primarily from rotations of the $ZnCl_4$ tetrahedra about the **c** axis, and has a wave vector $\mathbf{q}\simeq0.305\mathbf{c}^*$ just below $T_c\approx303$ K. The wave vector increases monotonically with decreasing temperature until ''locking-in'' to the commensurate value of $\mathbf{q}=\frac{1}{3}\mathbf{c}^*$ at a temperature $T_l\approx189$ K. The distortion in the incommensurate phase can be characterized by two components corresponding to the amplitude and phase of the modulation. Because there is no energy cost associated with a change in the phase of the modulation, this type of normal-incommensurate (N-IC) transition is a good experimental realization of phase transitions in the $n=2$, $D=3$ (3D-$XY$) universality class, free from the symmetry breaking perturbations often present in magnetic realizations of the model.

There have been several experimental studies of the N-IC phase transition in $Rb_2ZnCl_4$ and isomorphous materials.

 

TABLE I. Comparison of the critical exponents obtained for the N-IC transition in $Rb_2ZnCl_4$ from the present work with previous experimental results for transitions in the 3D-*XY* universality class, and with theoretical results. The theoretical values of the exponents $\beta_1$, $\gamma_1$, and $\nu_1$ are series expansion results, while $\beta_2$, $\beta_3$, and $\beta_4$ are obtained from $\beta_1$ via the scaling relation Eq. (1).

| Exponent | This work | $Rb_2ZnCl_4$ (Ref. 1) | Er (Refs. 8, 32, and 33) | Tm (Refs. 8 and 32) | Theory (Refs. 13 and 4) |
|---|---|---|---|---|---|
| $\beta_1$ | $0.35\pm0.01$ | $0.350\pm0.015$ | $0.47\pm0.05$ | $0.49\pm0.06$ | $0.345\pm0.005$ |
| $\beta_2$ | $0.87\pm0.01$ | $1.35\pm0.05$ | $0.97\pm0.10$ | $0.90\pm0.15$ | $0.886\pm0.013$ |
| $\beta_3$ | $1.50\pm0.04$ | $1.8\pm0.05$ | $1.80\pm0.30$ | | $1.61\pm0.02$ |
| $\beta_4$ | | | $2.2\pm0.3$ | $2.1\pm0.3$ | $2.49\pm0.04$ |
| $\gamma_1$ | $1.28\pm0.09$ | $1.26^{+0.04}_{-0.02}$ | $0.85\pm0.12$ | $0.90\pm0.04$ | $1.316\pm0.003$ |
| $\nu_1$ | $0.66\pm0.02$ | $0.683\pm0.015$ | $0.45\pm0.04$ | $0.43\pm0.02$ | $0.669\pm0.003$ |

There is general agreement between the measurements of $\beta_1$, the critical exponent of the primary order parameter: $\beta_1=0.350\pm0.015$ for $Rb_2ZnCl_4$ (x rays),[1] $\beta_1=0.30$ for $Rb_2ZnBr_4$ (neutrons),[2] and $\beta_1=0.375\pm0.025$ for $K_2SeO_4$ (neutrons).[3] In contrast, measurements of the exponent $\beta_2$, which characterizes the temperature dependence of the second harmonic, are inconsistent: $\beta_2=1.35\pm0.05$ for $Rb_2ZnCl_4$ (x rays),[1] $\beta_2\approx2\beta_1$ for $Rb_2ZnBr_4$ (neutrons),[2] and $\beta_2=0.785\pm0.035$ for $K_2SeO_4$ (neutrons).[3] The mean field theory result $\beta_2=2\beta_1$ can be modified by fluctuations, as shown by recent theoretical and experimental work on the scaling of secondary order-parameter critical exponents for transitions in liquid crystal systems, for which the transitions also belong to the 3D-*XY* universality class.[4] Brock *et al.*[5] measured the critical exponents of the successive sixfold Fourier components $C_{6n}$ of the bond orientational order in the smectic-C$\rightarrow$ tilted hexatic-I transition in the liquid crystal racemic 4-(2-methylbutyl)phenyl 4′, obtaining values in very good agreement with a multicritical scaling theory developed by Aharony *et al.*[4] which predicted for the $n$th harmonic that $\beta_n\sim\sigma_n\beta_1$, where

$$\sigma_n=n+x_n n(n-1), \tag{1}$$

and $x_n\simeq0.3-0.008n$. One aim of the present work was to test this theory to a higher degree of accuracy than has previously been attained for a solid-state system.

The behavior of the critical fluctuations of the secondary order parameters is also of great interest. Recently, Wu *et al.*[6] measured the critical scattering above $T_c$ at the primary and second harmonic satellite positions for the nematic-smectic-$A_2$ transition in the liquid crystal 7*APCBB*, and obtained different exponents for the correlation lengths of the fluctuations of the primary and secondary order parameters. This unexpected result was later explained by Aharony *et al.*,[7] who showed that the exponents were in fact the same, and that the apparent discrepancy was due to large deviations from the Lorentzian line shape at the second-harmonic position because of an unusually large susceptibility for the second-harmonic distortions.

The transitions from the paramagnetic phase to an incommensurate **c**-axis-modulated phase in the rare-earth metals Er and Tm are also believed to belong to the 3D-*XY* universality class. Recently, Helgesen *et al.*[8] have performed magnetic x-ray-scattering experiments on Er and Tm obtaining results (Table I) for the primary and secondary order parameter exponents $\beta_1-\beta_4$ which are, somewhat surprisingly, consistent with the mean-field exponents.

Further experiments are clearly needed to clarify the behavior of the secondary order parameters for the 3D-*XY* model. A high-resolution synchrotron x-ray-scattering study has the advantages that the high intensity allows the Bragg reflections to be measured over a wider range of temperature, while the good wave-vector resolution enables better discrimination of the Bragg scattering from the diffuse background. More accurate measurements than the previous studies of structural N-IC phase transitions should therefore be possible. The experiment also focused on the possible existence of scattering associated with two length scales above $T_c$. High-resolution x-ray- and neutron-scattering measurements have shown that this behavior occurs at a large number of phase transitions of both structural and magnetic character. As reviewed in Sec. IV, this is not yet understood, but both neutron- and x-ray-scattering studies have strongly suggested that the long length scale is associated with the ''near'' surface region of the crystal. Experiments to discover whether it occurs at structural N-IC phase transitions have not been performed to date. In these experiments, we show that two length scale behavior does occur at transitions of this type, and characterize the temperature dependence of the long length scale. By comparing the results of measurements made with different incident x-ray energies, we show that the long length scale scattering in these materials arises from the near-surface region.

In the next section of the paper we describe the experiments. Section III presents the results, which are discussed in Sec. IV.

## II. EXPERIMENT

The experiments were performed using four-circle diffractometers on the bending magnet beamline X20 and the wiggler beamline X17, of the National Synchrotron Light Source, Brookhaven National Laboratory, and on the undulator beamline TROIKA, of the European Synchrotron Radiation Facility.[9] The x rays were monochromated by double-bounce crystals with the Si(111) reflection giving an incident x-ray energy of 10.3 keV on X20, the diamond (111) reflection giving an energy of 15 keV on TROIKA, and the Si(220) reflection giving an energy of 60 keV on X17. Germanium (111) analyzer crystals were used on all three diffractometers to reduce background scattering and to

improve the scattered wave-vector resolution. The instrumental resolution was obtained from wave-vector scans through the primary incommensurate satellite well below $T_c$. Full widths of the principal axes of the resolution ellipsoid at half maximum intensity on X20 and X17 were typically $8\times10^{-4}$ Å$^{-1}$ and $2\times10^{-3}$ Å$^{-1}$ in the scattering plane, and $2\times10^{-2}$ Å$^{-1}$ out of plane, while for TROIKA the corresponding widths were approximately $4\times10^{-4}$ Å$^{-1}$, $2\times10^{-3}$ Å$^{-1}$, and $2\times10^{-2}$ Å$^{-1}$. Typical background intensities with the sodium iodide scintillation detectors used on the X20 and X17 diffractometers were $\sim10$ counts s$^{-1}$, while for the TROIKA diffractometer a germanium solid-state detector with energy analysis was used, and the typical background intensity was reduced to $\sim2$ counts s$^{-1}$.

The $Rb_2ZnCl_4$ single crystals were cleaved from a boule grown by the Czochralski technique by Gesland at the Université du Maine, with the **b** direction normal to a face (in the $Pmcn$ setting of the space group of the N phase, for which $a=7.285$ Å, $b=12.733$ Å, and $c=9.267$ Å). The measured mosaic spread was $\simeq0.01°$. An additional crystal used for the TROIKA experiment was grown by repeated recrystallization from aqueous solution[10] by Hamano, formerly of the Tokyo Institute of Technology, and had a mosaic spread of $<0.005°$, with the **a** direction normal to a face. The samples are colorless and transparent, and were etched with distilled water before the experiments.

For the X20 and TROIKA experiments the samples were mounted directly on the cold fingers of closed-cycle refrigerators, and the incident x rays were reflected from the sample surface. The x-ray penetration depth was $\sim10$ $\mu$m for both experiments, and so the scattering originates predominantly from the near-surface region of the crystal. The X17 experiment used a high incident energy, and the x rays were transmitted through the sample, which was mounted between Mylar sheets on the cold finger of a closed-cycle refrigerator. For the 60 keV photons used, the penetration depth is approximately equal to the 2 mm thickness of the crystal, and so the relative contribution to the total scattering from the near-surface region is smaller. The temperature was controlled to within 0.01 K in all experiments.

Calculations of satellite peak intensities were made for the low-temperature cell-tripled structure,[11] in order to identify particularly strong and weak reflections. Each experiment then began with a systematic search of the accessible reflections in order to find the most intense satellite peaks. The structure factor for the primary incommensurate satellite is zero in the $(h\ 0\ l)$ zone, and so the sample was mounted with the **b*** and **c*** reciprocal-lattice vectors in the scattering plane for the experiments using the X20 instrument. For the same reason the samples used for the experiments on the X17 and TROIKA instruments were initially mounted with the **a*** and **b*** reciprocal-lattice vectors in the scattering plane for most of the measurements. The four circle geometry was exploited to allow the momentum transfer to be scanned in the **c*** direction.

## III. EXPERIMENTAL RESULTS

### A. Determination of $T_c$

One of the most difficult problems in the precise study of critical scattering is the determination of the transition temperature. We have used two different approaches. First, as pointed out by Bruce,[12] $T_c$ can be located accurately by a measurement of the temperature derivative of the total scattered intensity at a primary incommensurate satellite position. The divergence of the correlation length at $T_c$ means that sufficiently close to $T_c$, the finite instrumental resolution effectively integrates over the scattering from all the critical fluctuations. The measured scattering therefore has the same temperature dependence as the energy, and the temperature derivative of the total intensity is proportional to the critical contribution to the specific heat. Figure 1 shows the intensity measured with the momentum transfer scanned in the **c*** direction through the $(-1\ 8\ -1+q)$ incommensurate satellite at a temperature $T_c-0.6$ K, using the X20 instrument. The solid line is a fit to the data using a Lorentzian +Lorentzian-squared line shape, which has no particular significance other than that it was found to give a good description of the data. The numerically evaluated temperature derivative of the integrated intensity, $dI/dT$, obtained from similar scans is shown in Fig. 2, and has a well-defined peak at $T_c=(303.4\pm0.05)$ K. This method was also used to determine the transition temperatures of the samples used for the X17 ($T_c=303.6\pm0.05$ K) and TROIKA ($T_c=302.8\pm0.05$ K) experiments. Since the samples used for the X20 and X17 experiments were cut from the same boule, the 0.2 K difference in measured transition temperatures is probably due to calibration differences between the two temperature sensors. As discussed above, the sample used for the TROIKA experiment was grown by a different technique, and the slightly lower transition temperature probably reflects this, in addition to possible calibration differences.

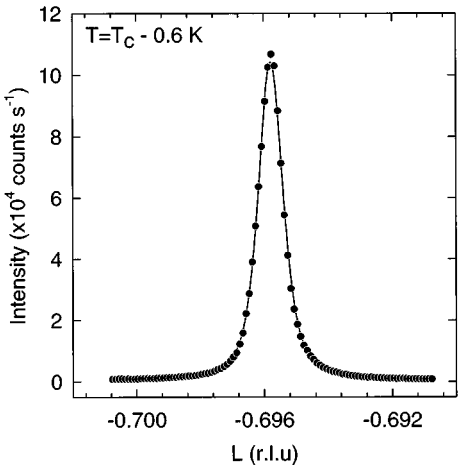


FIG. 1. Scan through the $(-1\ 8\ -1+q)$ incommensurate peak position at a temperature $T_c-0.6$ K using the X20 diffractometer. The solid line is a fit to the data of a Lorentzian+Lorentzian-squared line shape as discussed in the text.

The second method used to determine $T_c$ was to measure the diffuse scattering above $T_c$ as a function of temperature, at a reciprocal-lattice position $\mathbf{q}+\delta$, where $\mathbf{q}$ is an incommensurate peak position. Extrapolating the temperature at which the diffuse scattering is a maximum for a given value of $\delta$ to $\delta=0$ gives the critical temperature, because the width of the diffuse scattering is a minimum at $T_c$. Figure 3 shows the diffuse scattering close to the $(-1\ 8\ -1+q)$ primary

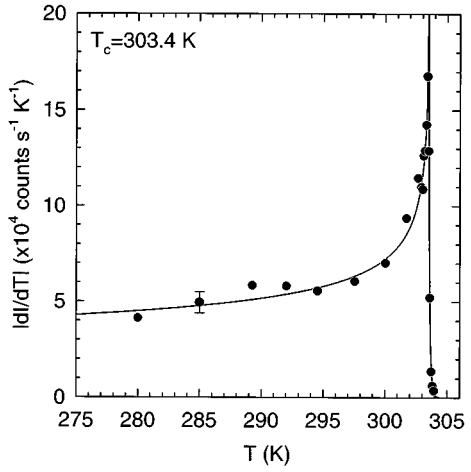


FIG. 2. The derivative of the total integrated intensity at a primary incommensurate satellite position exhibits a cusp at $T_c$, allowing accurate location of the transition temperature. These data were obtained from scans through the $(-1\ 8\ -1+q)$ primary satellite obtained with the X20 diffractometer. A typical error bar is shown.

satellite, measured using the X20 instrument. The broken line shows the locus of the position of the maximum in the diffuse scattering. Extrapolation to $\delta=0$ gives $T_c=(303.4\pm0.1)$ K, in agreement with the value obtained above.

The first method makes a virtue of poor wave-vector resolution, as a large resolution volume integrates the scattering from all the critical fluctuations over a correspondingly greater temperature range. In practice, experimental uncertainties make interpolation of the position of the peak in $dI/dT$ difficult, and so it is necessary to take data in fine temperature increments close to the transition. The second method relies on the accurate measurement of the inherently weak diffuse scattering, and the extrapolation procedure may introduce uncertainty into the final result. We consider that the first method is both easier to use, and more accurate.

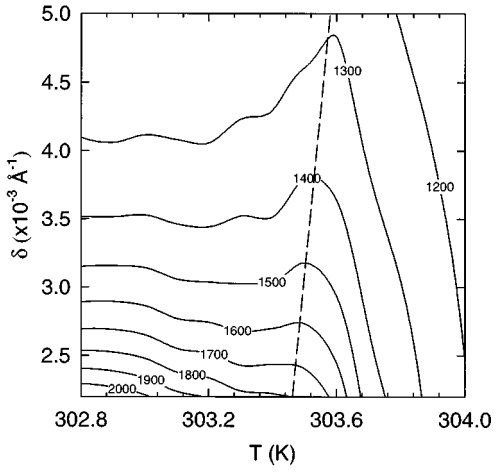


FIG. 3. Contour plot of the diffuse scattering measured at $(-1\ 8\ -1+q+\delta)$ as a function of temperature, using the X20 instrument. The broken line is a fit to the temperature positions of the maxima in the diffuse scattering at each value of $\delta$. Extrapolation to $\delta=0$ gives $T_c=303.4\pm0.1$ K.

### B. Critical exponents for the incommensurate order parameters

The development of the incommensurate modulation below $T_c$ leads to the appearance of satellite peaks around the main Bragg peaks at reciprocal-lattice positions $\mathbf{G}_{hkl}\pm n\mathbf{q}$, where $\mathbf{G}_{hkl}$ is a reciprocal-lattice vector of the high-temperature phase. The temperature dependence of the reflections for $n=1$, 2, and 3 was measured with the diffractometer on X20, by scanning the momentum transfer in the $\mathbf{c}^*$ direction through the $(-1\ 8\ -1+q)$, $(-1\ 8\ -2+2q)$, $(0\ 8\ -2q)$, and $(-1\ 8\ -1+3q)$ satellites. The data was fitted as shown in Fig. 1, and the integrated intensity obtained.

Scattering from order parameter fluctuations can make a significant contribution to the observed intensity close to $T_c$, where the Bragg scattering is weak. In general, this fluctuation scattering must be subtracted from the data if reliable values of the critical exponents $\beta_n$ are to be obtained. This difficulty is lessened by good wave-vector resolution, but it is always a problem very close to $T_c$. Usually an approximation to the fluctuation scattering below $T_c$ is deduced from the scattering above $T_c$, where the intensity of the Bragg scattering is identically zero. We adopt the phenomenology of Majkrzak *et al.*[3] and approximate the fluctuation scattering below $T_c$ by

$$I(-t)=\tfrac{1}{2}I(0)+\tfrac{1}{2}I(2t). \tag{2}$$

The motivation for this approximation is that the first term on the right-hand side of Eq. (2) corresponds to the scattering from a temperature-independent phason mode, and the second to an amplitude mode hardening below $T_c$ with an amplitude ratio of about 2. Although Eq. (2) is undeniably approximate, the high wave-vector resolution of the present experiment means that the corrections to the observed intensity of the scattering at the primary satellite position are relatively small, and neglecting them entirely alters the resulting value of the exponent by only about 3%. The scattering above $T_c$ at the secondary satellite positions was so weak that it could not be reliably measured, and so no correction to the intensities below $T_c$ was made. Measured intensities at the $1q$, $2q$, and $3q$ incommensurate satellite positions are plotted in Fig. 4.

Close to $T_c$, the intensity of the $n$th-order satellite is proportional to the square of the $n$th-order parameter, and in the critical region the intensities are therefore proportional to a simple power law

$$I_n=A_n|t|^{2\beta_n}, \tag{3}$$

where $t$ is the reduced temperature $t\equiv(T/T_c)/T_c$. The continuous lines in Fig. 4 are fits of Eq. (3) to the intensities with the critical temperature fixed at $T_c=303.4$ K. The resulting values of $\beta_n$ are tabulated in Table I.

Finally, we comment that at structural phase transitions there are two contributions to the scattering for $n>1$. The first arises from one-phonon scattering by the higher Fourier components of the structural distortion, which form a class of secondary order parameters for the transition, and the second from higher-order diffraction harmonics (many-phonon scattering from the primary distortion), and is present even if the distortion is perfectly sinusoidal. Asymptotically, both

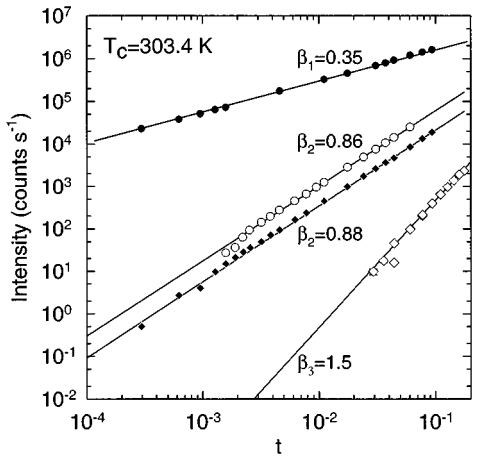


FIG. 4. Temperature dependence of incommensurate satellite peak intensities. Open squares are intensities obtained from **c*** direction scans through the $(2\ -3\ 4-q)$ satellite using the X17 instrument. The remaining data were obtained from **c*** direction scans using the X20 instrument. Filled circles are from scans through the $(-1\ 8\ -1+q)$ peak, open circles from scans through the $(0\ 8\ -2q)$ peak, filled diamonds from scans through the $(-1\ 8\ -2+2q)$ peak, and open diamonds from scans through the $(-1\ 8\ -1+3q)$ peak. Solid lines are fits to the data of power laws of the form $I=A|t|^{2\beta_n}$.

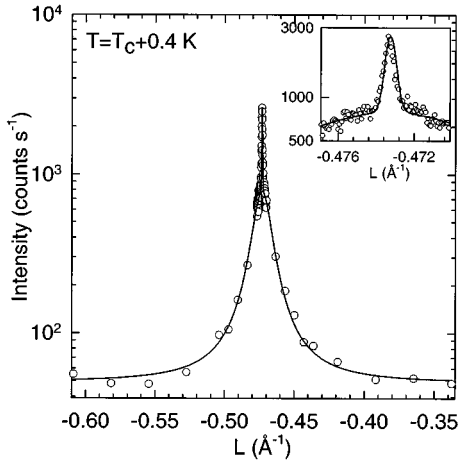


FIG. 5. Critical scattering measured at $T_c+0.4$ K at the $(-1\ 8\ -1+q)$ primary incommensurate satellite position, using the X20 instrument. The inset is an enlargement of the central region of the main graph, and clearly shows the long length scale component of the scattering discussed in the text. The solid line is a fit to the data of a Lorentzian+Lorentzian-squared line shape convoluted with the instrumental resolution function, as discussed in the text.

processes depend on the same correlation functions, and so have the same temperature dependence, even though a detailed explanation of the magnitude of the amplitudes of the scattering would require detailed knowledge of both effects.

### C. Critical scattering above $T_c$

The critical scattering above $T_c$ was measured by scanning the momentum transfer in the **c** direction through the $(-1\ 8\ -1+q)$ satellite on the X20 instrument, in the **a*** and **b*** directions through $(6\ 0\ 1+q)$ on the TROIKA instrument, and in the **b*** and **c*** directions through $(2\ -3\ 4-q)$ on the X17 instrument. Typical results are shown in Figs. 5–7. As shown in Fig. 5, the X20 data clearly exhibit a two-component line shape at $T_c+0.4$ K, with a nearly resolution limited sharp component superposed on a considerably broader diffuse component. Figure 6 indicates that a similar cross section was observed with the TROIKA instrument, and that the sharp component was only observed between $T_c$ and $T_c+1.4$ K. In contrast the data taken with high energy, 60 keV x rays using the X17 instrument, displayed in Fig. 7, show only a single component line shape.

Further analysis requires the scattering to be modeled. We have used the model that has proved successful in other materials showing the two-length scale behavior: namely an anisotropic Lorentzian form to describe the broad component, an isotropic Lorentzian-squared form for the sharp component, and a constant background:

$$I(\mathbf{q})=\chi_0\left[1+\sum_i\left(\frac{q_i}{\kappa_i}\right)^2\right]^{-1}+\chi_0^{(s)}\left[1+\left(\frac{q}{\kappa^{(s)}}\right)^2\right]^{-2}+A. \tag{4}$$

The instrumental resolution function was assumed to be triangular in the out-of-scattering plane direction, and Gaussian in the in-plane directions. This functional form was fitted to scans through the primary incommensurate satellite well below $T_c$, in order to determine the widths of the triangular and Gaussian components. The scattering model [Eq. (4)] was convoluted with the parametrized instrumental resolution; the out-of-plane convolution was performed analytically, and the in-plane convolution was performed numerically using a two-dimensional Gauss rule algorithm.

Measurements well above $T_c$, where the effects of the finite resolution and the intensity of the sharp component are both negligible, show that the inverse correlation lengths in the **c*** direction are approximately a factor of 2 greater than those in the **a*** and **b*** directions, in agreement with previ-

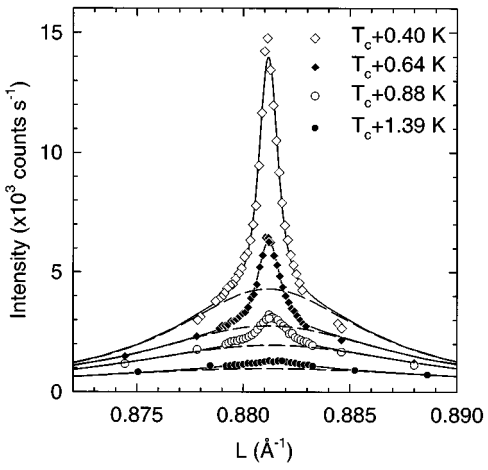


FIG. 6. Central portion of scans through the incipient $(6\ 0\ 1+q)$ primary incommensurate satellite obtained using the TROIKA instrument, showing the long length scale component in the critical scattering above $T_c$. The solid lines are fits to the data of the resolution convoluted scattering function [Eq. (4)] discussed in the text. The broken lines show the Lorentzian components of the fits alone.

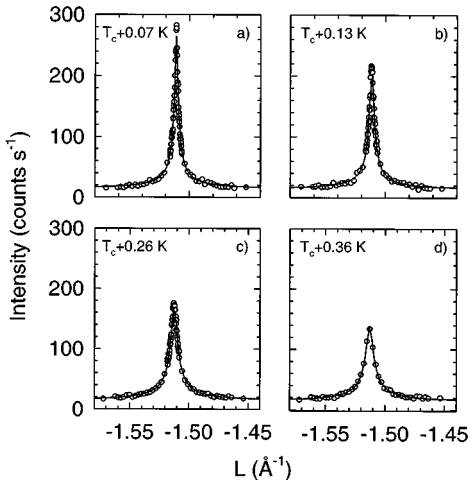


FIG. 7. Scans through the $(2\ -3\ 4-q)$ primary incommensurate satellite position above $T_c$, measured with an incident energy of 60 keV using the X17 instrument. The solid lines are fits to the data of a Lorentzian line shape convoluted with the instrumental resolution. Any second length scale component is clearly weak, if present at all.

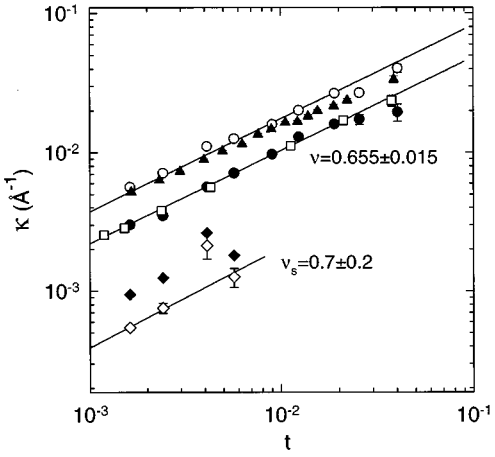


FIG. 8. Widths of the diffuse scattering above $T_c$ extracted from fits to scans through incipient primary incommensurate satellite peaks, as described in the text. Open circles are the widths $\kappa_c$ of the short length scale component from **c*** direction scans through the $(6\ 0\ 1+q)$ satellite using the TROIKA instrument, and the filled circles are corresponding widths $\kappa_a$ from **a*** direction scans. Solid triangles are the widths $\kappa_c$ from scans through the $(-1\ 8\ -1+q)$ satellite using the X20 instrument, and open squares show the widths $\kappa_b$ from **b*** direction scans through the $(2\ -3\ 4-q)$ satellite using the X17 instrument. Open and filled diamonds show the widths of the long length scale component $\kappa^{(s)}$ extracted from **c*** direction scans with and without the resolution convolution, respectively.

ous measurements.[1] It has therefore been assumed that $\kappa_a=\kappa_b=\frac{1}{2}\kappa_c$ in Eq. (4). The instrumental resolution prohibited a reliable estimate of the width of the sharp component except in the highest resolution direction. However, studies on other compounds have indicated that the sharp component is approximately isotropic, and so in the absence of more detailed information we have assumed that this is the case in $Rb_2ZnCl_4$. In fact, the widths obtained for the sharp component are not very sensitive to this assumption: assuming that the sharp component has the same anisotropy as the broad component, for example, changed the widths given by the fits (and the resulting exponents) by less than the corresponding uncertainties. At each temperature, the values of $\chi_0$, $\kappa_c$, $\chi_0^{(s)}$, and $\kappa^{(s)}$ which best fitted the data were found. The background term, $A$, was held to the same value for all temperatures. In all cases, the fits gave a good description of the data ($\chi^2\sim 1$–4), as shown in Figs. 5 and 7.

Before discussing the results obtained from these fits it is worth commenting on the extent to which the results are sensitive to the details of the assumed functional form and the resolution function. Usually, as in the present analysis, an assumed form of the intrinsic scattering is convoluted with the measured instrumental resolution, and the result fitted to the data. However, when one (or more) of the widths of the intrinsic scattering becomes comparable to the corresponding width of the resolution function, the result of the convolution can be very sensitive to the detailed form assumed for both the resolution function and the intrinsic scattering. Because the resolution perpendicular to the scattering plane is typically two orders of magnitude larger than the in-plane resolution this difficulty persists over a large temperature range. It is therefore important to characterize the critical scattering and resolution function in all three dimensions if accurate parameter estimation is required. For example, if an isotropic scattering function is assumed [$\kappa_a=\kappa_b=\kappa_c$ in Eq. (4)], and $T_c$ estimated from a power-law fit to the amplitudes $\chi_0$ extracted from the fits, a value $\sim 0.5$ K lower than that obtained in Sec. III A is found. If the same procedure is performed with the correct anisotropy, $\kappa_a=\kappa_b=\frac{1}{2}\kappa_c$, the resulting value of $T_c$ is consistent with the value obtained in Sec. III A to within the experimental uncertainties. For this reason alone it is essential to have an independent measurement of the critical temperature.

The presence of a second component in the scattering makes the problem of accounting for the effects of the instrumental resolution particularly difficult close to $T_c$, where both components become resolution limited. The proportion of the total scattering associated with each component becomes poorly defined, because the line shape of the observed scattering is dominated by the resolution function, rather than by the intrinsic scattering. Accurate parameter estimation is then particularly difficult.

The results for the inverse correlation lengths are shown in Fig. 8. The results are in good mutual agreement, and fits to a power law

$$\kappa\sim t^{\nu}$$

with $T_c$ fixed to the observed values give $\nu=0.655\pm 0.015$ (TROIKA), $\nu=0.68\pm 0.01$ (X17), and $\nu=0.62\pm 0.03$ (X20), in agreement with the series expansion 3D-$XY$ value $\nu=0.669\pm 0.003$.[13]

In a similar manner, the intensity of the broad component, $\chi_0$, is shown in Fig. 9 as a function of temperature. The continuous lines are fits to the data of power laws

$$\chi_0\sim t^{\gamma}$$

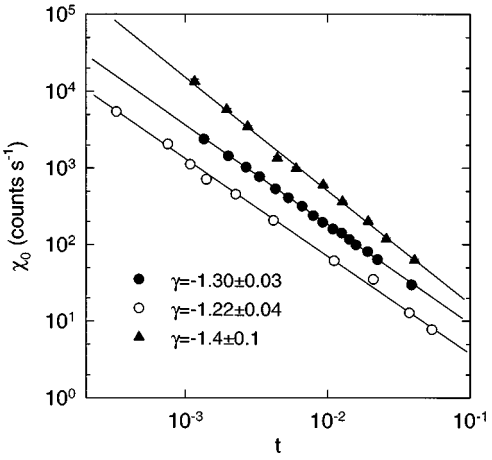


FIG. 9. Peak amplitudes of the broad components of the critical scattering above $T_c$. Filled triangles are amplitudes obtained from fits to **c*** direction scans through the $(6\ 0\ 1+q)$ satellite position using the TROIKA instrument. Filled circles are intensities obtained from **c*** direction scans through the $(-1\ 8\ -1+q)$ satellite position using the X20 instrument, and open circles are intensities obtained from **c*** direction scans through the $(2\ -3\ 4-q)$ satellite position using the X17 instrument. Solid lines are fits to the data of power laws of the form $I\sim|t|^{\gamma}$, as discussed in the text.

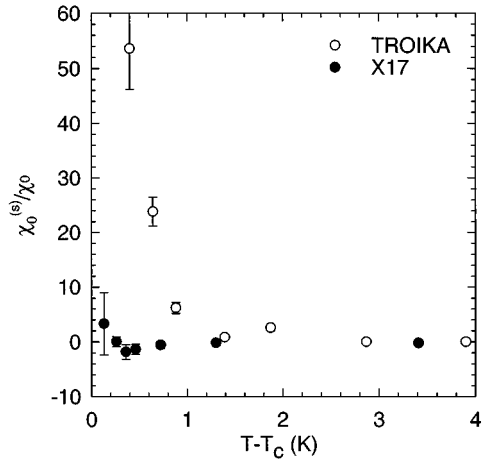


FIG. 10. Ratio of the amplitudes of the long and short length scale components. Open circles are the ratios obtained from fits to **c*** direction scans through the $(-1\ 8\ -1+q)$ satellite position using the X20 diffractometer with an incident x-ray energy of 10.3 keV. Filled circles are the ratios obtained from fits to **c*** direction scans through the $(2\ -3\ 4-q)$ satellite position using the X17 diffractometer in transmission geometry, with an incident x-ray energy of 60 keV.

with $\gamma=1.4\pm0.1$ (TROIKA), $\gamma=1.22\pm0.04$ (X17), and $\gamma=1.30\pm0.03$ (X20), in agreement with the theoretical 3D-$XY$ value $\gamma=1.316\pm0.005$.[13]

Unlike the results obtained with a low incident energy (Figs. 5 and 6), the 60 keV incident energy X17 data (Fig. 7) show no obvious evidence of a two component line shape. The continuous line represents a fit to the data of a Lorentzian-only line shape [$\chi_0^{(s)}=0$ in Eq. (4)] convoluted with the resolution function; a two component line shape does not significantly improve the fit to the data ($\chi^2$ is only reduced from 2.4 to 2.1). The ratio of sharp to broad component amplitudes, $\chi_0^{(s)}/\chi_0$, for the TROIKA and X17 experiments is shown in Fig. 10, and demonstrates that while a strong sharp component develops in the data from the low incident energy TROIKA experiment as $T_c$ is approached from above, no such scattering is observed in the data obtained with high incident energy in the X17 experiment. These results support the hypothesis that the sharp component scattering arises in the ''near''-surface region for the N-IC transition in $Rb_2ZnCl_4$, as suggested by the results of neutron- and x-ray-scattering experiments on the magnetic phase transitions in Ho (Refs. 14,15) and Tb,[16] and the paradigmatic soft-mode transition in $SrTiO_3$.[17] It is evident from Fig. 10 that the exponent $\gamma_s$ for the sharp component amplitude is considerably greater than the broad component exponent, and fits to the data yield $\gamma_s=4\pm1$. However, the amplitudes of the sharp component are extremely sensitive to the details of the resolution function, and although the resulting exponent is less so, the exponent is not well determined.

Measurements were attempted of the critical scattering at secondary satellite positions, but the intensity was simply too low to be measured reliably, even very close to $T_c$. The intensity of the $n$th-order parameter critical scattering is, at least in part, proportional to the bare susceptibility of the $n$th harmonic—the value of the susceptibility in the absence of coupling to the primary order parameter.[7] As there is no reason to expect modes with wave vectors $n\mathbf{q}$ to soften close to $T_c$ (or indeed at all), the susceptibility of the higher harmonic peaks is expected to be very small, not only for $Rb_2ZnCl_4$, but in general.

## IV. DISCUSSION AND CONCLUSIONS

### A. Critical exponents

As discussed above, the N-IC transition in $Rb_2ZnCl_4$ belongs to the universality class of a $D=3$ $XY$ system, and so it is of interest to compare the results both with theoretical predictions for this universality class, and with other experimental determinations of the exponents for systems believed to belong to this class. The measurements were performed with high wave-vector resolution on synchrotron x-ray sources at the NSLS and ESRF, and so it is also of interest to compare with those obtained using laboratory x-ray sources by Andrews and Mashiyama.[1] The resolution widths in the experiment of Andrews and Mashiyama was 5–10 times larger in the scattering plane, and five times larger perpendicular to that plane, than that of the present work. Their measurements of the order-parameter amplitude, $\beta_1$, covered the reduced temperature range $t=0.005$ to 0.1, whereas the corresponding range in our experiments was $t=0.0003$ to 0.1. Above $T_c$, they collected data from $t=0.001$ to 0.1 as in these experiments. The results of both experiments are summarized in Table I, and for $\beta_1$, $\nu_1$, and $\gamma_1$, the agreement between the two sets of results is excellent, as is the agreement with the results of series-expansion calculations and experimental results for liquid crystals.[5,6] Table I also shows that these results disagree with the measured exponents of Er and Tm, whose magnetic phase transitions are also expected to belong to the 3D-$XY$ universality class.

The high intensity and high resolution of the present experiments enabled measurements of the temperature depen-

dence of the scattering at the higher harmonics to be made to reduced temperatures down to $3\times10^{4}$ ($\beta_2$) and $3\times10^{-2}$ ($\beta_3$), whereas Andrews and Mashiyama's measurements were made only for $t>0.1$. The results we obtain agree well with theory, and with experiments on liquid crystals, but not with those of Andrews and Mashiyama. We suspect that this is partly because they were unable to perform measurements sufficiently close to $T_c$, and partly because they chose a particularly weak second-order satellite for study. We consider, therefore, that our results for $\beta_2$ and $\beta_3$ are to be preferred, and show that the theory for the higher-order exponents developed by Aharony *et al.*[4] applies not only to liquid crystals, but also to $Rb_2ZnCl_4$.

Even so, we were not be able to measure the critical fluctuations above $T_c$ at a second-order Bragg reflection. Since the susceptibility is likely to be small at $2\mathbf{q}$, this is not surprising, and lends support to the suggestion by Aharony *et al.*[7] that the anomalous behavior observed by Wu *et al.*[6] is due to the exceptionally large susceptibility at $2\mathbf{q}$ in the liquid crystal system they studied. In conclusion, the behavior of the broad component of the critical scattering, and of the order parameters in $Rb_2ZnCl_4$ are in excellent agreement with theoretical predictions for the 3D-$XY$ universality class.

### B. The long length scale

Although the 3D-$XY$ model gives a good description of most of our results for the critical scattering from $Rb_2ZnCl_4$, it fails to explain the two component line shape observed just above $T_c$. Andrews and Mashiyama[1] did not observe this line shape because the instrumental resolution in their x-ray experiment was too poor to be able to distinguish the two components. Nevertheless, similar results have now been observed with high-resolution x-ray or neutron scattering at a variety of structural and magnetic phase transitions. Indeed, there are few examples of sufficiently high wave-vector resolution critical scattering experiments performed on crystals in which a two component line shape has not been seen. Initially we review the experimental results obtained for the long length scale component in Sec. III, and compare them with those for other materials.

(1) The long length scale component in $Rb_2ZnCl_4$ is observed to be an appreciable fraction of the total critical scattering only very close to $T_c$ ($t<0.005$). A similarly small temperature range is found for the structural phase transitions of the perovskite materials,[18–21] and for the magnetic phase transitions of the rare-earth metals and actinides.[14–16,22,23]

(2) The scattering associated with the long length scale is approximately isotropic in reduced wave vector, and is consistently described by an isotropic Lorentzian-squared cross section. In other materials, the scattering has also been described by an isotropic Lorentzian-squared line shape, or is more isotropic than the broad component of the scattering.[15,18–21,24]

(3) The exponents describing the temperature dependence of the inverse correlation length, $\nu_s$, and susceptibility, $\gamma_s$, are $0.7\pm0.2$ and $4\pm1$, respectively. These can be compared with similar measurements on $SrTiO_3$ (Ref. 19) ($\nu_s=0.5\pm0.09$ and $\gamma_s=2.6\pm0.15$), $CuGeO_3$ (Ref. 24) ($\nu_s=0.56\pm0.09$, and $\gamma_s=2.0\pm0.3$), $RbCaF_3$ (Ref. 21) ($\nu_s=0.60\pm0.08$) and the magnetic transition of Ho ($\nu_s=0.95\pm0.1$, and $\gamma_s=4\pm1$).[14,15]

(4) The long length scale is $\sim10$ times the correlation length of the broad component of the scattering. This is approximately the case for all materials for which the length scales have been measured.

(5) Evidence that the long length scale scattering originates in the near-surface region of the crystal is provided by the observation that it is a less significant part of the scattering measured with high-energy 60 keV x rays for which the penetration depth is $\sim$mm than with low-energy 15 keV x rays, for which the penetration depth is $\approx10$ $\mu$m. Similar results have been obtained for $SrTiO_3$,[17] and for rare-earth metals using narrow beams of neutrons.[15,16] Experiments have also shown that the long length scale component is changed if the sample surface is scratched, polished, or etched, with the rougher surfaces tending to give a larger proportion of long length scale scattering.[15,18–22]

(6) Experiments on $RbCaF_3$ and $KMnF_3$ which have slightly first-order phase transitions have shown that the long length scale component is strained, even though above $T_c$ the bulk crystal is unstrained. Indeed, in $Rb_2ZnCl_4$ and all of these systems, there is a strong coupling between the primary order parameter and the macroscopic strains. It is worth noting that similar experiments on liquid crystals,[6] which cannot support strain fields, have not observed two length scale behavior.

The above summary provides a brief account of the main points of the experimental results which have so far been obtained on the long length scale components of the critical scattering at phase transitions. We now describe some of the theories that have been put forward to explain these results.

(1) Close to a first-order phase transition both phases can be stable, particularly if the crystal contains defects, and so is not homogeneous. Because the first system in which the phenomena was observed were perovskites in which the structural phase transition is slightly first order ($RbCaF_3$ and $KMnF_3$), or may be weakly first order ($SrTiO_3$), it was suggested, following Imry and Wortis,[25] that the two length scales arise because different parts of the crystal are in each of the two phases. Subsequently, the phenomena has been observed in many materials for which the transitions are clearly continuous and so this suggestion seems inapplicable, at least without further modification.

(2) The phenomena has been shown to occur in the near-surface region and so one possibility is that it is surface induced. It is well known that the surface layers of a crystal may have a new structure and different interatomic distances. This will lead to changes in the interatomic forces of the top few layers, so that the transition might occur at a higher temperature at the surface than in the bulk. Detailed theories[26] of how this order propagates into the bulk when the system is smooth, and as the temperature is lowered suggest that once the ordering has propagated to a greater depth than the distorted planes, it follows the bulk correlation length. Since the long length scale is found to be roughly isotropic, very long ($\sim1000$ Å), and very different from the bulk correlation length perpendicular to the surface, this type of theory cannot explain the results. It seems unlikely that real surfaces are sufficiently rough on the 1000 Å scale to change qualitatively the results of such theories.

(3) There have been two different proposals based on the hypothesis that there are extended defects in the near-surface region which modify the critical phenomena and lead to the second length scale. Altarelli *et al.*[27] suggested that the defects produce random bond disorder which decays with distance like $|r|^{-a}$. They then made use of the work by Weinrib and Halperin,[28] who showed that if $a<d$ the critical phenomena are different from those of the pure system, with very different exponents: $\nu_s=2/a$ and $\gamma_s=4/a$ for point defects, and, presumably, that $T_c$ is also slightly different. They suggested that in the near-surface region there are dislocations which produce the necessary long-range correlations in the defects, with $a=2$. This theory fails, however, to explain the Lorentzian-squared profile, or why the scattering is so isotropic, because if the dislocations are due to the surface preparation, they might be expected to lie in particular planes.

The second proposal is to argue that random fields generated by near-surface defects play a significant role (Harris *et al.*[24]). In this case, the scattering consists of both a connected and a disconnected part, with a Lorentzian and a Lorentzian-squared form, respectively. The theory of critical phenomena then states that the correlation lengths of both parts must scale with the same exponents, as found for random staggered fields in antiferromagnets.[29] Harris *et al.* suggest that the difference in absolute magnitudes of the two length scales might arise because of the extended nature of the defects in these systems, although exactly how this happens is unclear. The susceptibility exponent $\gamma_s=(4-\eta_s)\nu_s$ with $0\leqslant\eta_s\leqslant 1$ for a continuous transition so that $\gamma_s=4\nu_s$ is the maximum value. The unexplained features of this proposal are that the extended defects are unlikely to be isotropic, the explanation of the two length scales needs to be developed, and the exponents of at least some systems seem to be inconsistent with the predictions.

(4) We suggest a fourth explanation, based partly on the observation that the strain appears to play an important role. The theory of phase transitions of compressible lattices was discussed by Wegner,[30] and by Bergman and Halperin,[31] who showed that strains at the surface would only penetrate into the bulk by a distance approximately equal to the correlation length. Consequently, it was concluded that for macroscopic samples the coupling between the strains and the order parameter could be neglected above $T_c$. This is not the case, however, for experiments which are sensitive to the surface of crystals. The surface elastic waves can allow fluctuations near to the surface to behave as if the crystal were free rather than clamped against strain relaxation. Since the effective interaction between the fluctuations is different and weaker in a free crystal than in a clamped crystal, the fluctuations close to the surface will behave as if the reduction in $T_c$ is less than that for fluctuations in the bulk. These near-surface free fluctuations will then have a longer correlation length and larger amplitude than the bulk clamped fluctuations. We have been unable to work out the detailed consequences of this proposal for the detailed scattering cross section or for the critical exponents. Nevertheless, the proposal does provide a natural explanation for two length scales in pure crystals of any form. It does explain the near-surface nature of the long length scale, and since the surface elastic waves depend on the boundary conditions, the second length scale component would be expected to be affected by surface preparation. Furthermore, the isotropic behavior of the long length scale might result because the penetration depth of the surface waves in an elastically isotropic medium is given by their wavelength along the surface. Finally, this theory predicts that the two length scale phenomena should not occur if the transition is described by mean-field theory, or if the coupling between the order parameter and the strain is negligible.

(5) A final, if unlikely, proposal is that the scaling theory of phase transitions is wrong, and that it is not possible to describe the fluctuations by a single length scale. Given the enormous success of scaling theory, this proposal can only be seriously considered once all other, less drastic, proposals have been ruled out.

At present we are unable to determine whether any of these proposals are the correct explanation of the observed phenomena. More experimental results are also needed to understand the dependence on the surface preparation and to discover whether there are extended defects throughout the near-surface region. More detailed experiments are needed to provide sufficiently accurate measurements of the exponents to see if they agree with any of the models, and to study the isotropy and line shape of the long length scale component of the scattering. Furthermore, we need to know if the same phenomena occur in systems where there is negligible coupling to strains, such as $MnF_2$ or Gd, and whether they occur in systems such as potassium dihydrogen phosphate that are well described by mean-field theory. Further work is also needed to develop the theoretical predictions, both for the theories dependent upon defects, and for the proposal based on strains. We hope that our results will help to stimulate this work.

## ACKNOWLEDGMENTS

We would like to thank J. B. Hastings, D. P. Siddons, and Doon Gibbs for help with the NSLS experiments, and K. Hamano and H. Mashiyama for supplying one of the samples used for the ESRF experiment. The work carried out at Brookhaven National Laboratory is supported by the U.S. DOE under Contract No. DEA-C02-CH00016, and that at Oxford and the ESRF by financial support from the EPSRC.

[1] S. R. Andrews and H. Mashiyama, J. Phys. C **16**, 4985 (1983).

[2] C. J. De Pater and C. Van Dijk, Phys. Rev. B **18**, 1281 (1978).

[3] C. F. Majkrzak, J. D. Axe, and A. D. Bruce, Phys. Rev. B **22**, 5278 (1980).

[4] Amnon Aharony, R. J. Birgeneau, J. D. Brock, and J. D. Litster, Phys. Rev. Lett. **57**, 1012 (1986).

[5] J. D. Brock, A. Aharony, R. J. Birgeneau, K. W. Evans-Lutterodt, J. D. Litster, P. M. Horn, G. B. Stephenson, and A. R. Tajbakhsh, Phys. Rev. Lett. **57**, 98 (1986).

[6] Lei Wu, M. J. Young, C. W. Garland, R. J. Birgeneau, and G.

Heppke, Phys. Rev. Lett. **72**, 376 (1994).
[7] Amnon Aharony, R. J. Birgeneau, C. W. Garland, Y. -J. Kim, V. V. Lebedev, R. R. Netz, and M. J. Young, Phys. Rev. Lett. **74**, 5064 (1995).
[8] G. Helgesen, J. P. Hill, T. R. Thurston, and D. Gibbs, Phys. Rev. B **52**, 9446 (1995).
[9] G. Grübel, J. Als-Nielsen, and A. K. Freund, J. Phys. (Paris) Colloq. **55**, C-94 (1994).
[10] K. Hamano, H. Sakata, K. Yoneda, K. Ema, and S. Hirostsu, Phase Transitions **11**, 279 (1988).
[11] K. Itoh, A. Hinasada, M. Daiki, and J. N. Nakamura, J. Phys. Soc. Jpn. **58**, 2070 (1989).
[12] Alistair D. Bruce, J. Phys. C **14**, 193 (1981).
[13] J. C. Le Guillou and J. Zinn-Justin, Phys. Rev. B **21**, 3976 (1981).
[14] T. R. Thurston, G. Helgesen, Doon Gibbs, J. P. Hill, B. D. Gaulin, and G. Shirane, Phys. Rev. Lett. **70**, 3151 (1993).
[15] T. R. Thurston, G. Helgesen, J. P. Hill, Doon Gibbs, B. D. Gaulin, and P. J. Simpson, Phys. Rev. B **49**, 15 730 (1994).
[16] P. M. Gehring, K. Hirota, C. F. Majkrzak, and G. Shirane, Phys. Rev. Lett. **71**, 1087 (1993).
[17] H. B. Neumann, U. Rütt, R. Schneider, and G. Shirane, Phys. Rev. B **52**, 3981 (1995).
[18] S. R. Andrews, J. Phys. C **19**, 3721 (1986).
[19] D. F. McMorrow, N. Hamaya, S. Shimomura, Y. Fujii, S. Kishimoto, and H. Iwasaki, Solid State Commun. **76**, 443 (1990).
[20] A. Gibaud, R. A. Cowley, and P. W. Mitchell, J. Phys. C **20**, 3849 (1987).
[21] U. J. Nicholls and R. A. Cowley, J. Phys. C **20**, 1987 (1987).
[22] G. M. Watson, B. D. Gaulin, Doon Gibbs, G. H. Lander, T. R. Thurston, P. J. Simpson, Hj. Matzke, S. Wang, M. Dudley, and S. M. Shapiro, Phys. Rev. B **53**, 686 (1996).
[23] S. C. Perry, W. J. Nuttall, W. G. Stirling, G. H. Lander, and O. Vogt (unpublished).
[24] Q. J. Harris, Q. Feng, R. J. Birgeneau, K. Hirota, G. Shirane, M. Hase, and K. Uchinokura, Phys. Rev. B **52**, 15 420 (1995).
[25] Yosef Imry and Michael Wortis, Phys. Rev. B **19**, 3580 (1979).
[26] K. Binder, *Phase Transitions and Critical Phemomena* (Academic, New York, 1984), Vol. 8, p. 1.
[27] M. Altarelli, M. D. Nuñez Regueiro, and M. Papoular, Phys. Rev. Lett. **74**, 3840 (1995).
[28] A. Weinrib and B. I. Halperin, Phys. Rev. B **27**, 413 (1983).
[29] R. A. Cowley, G. Shirane, H. Yoshizawa, Y. J. Uemura, and R. J. Birgeneau, Z. Phys. B **75**, 303 (1989).
[30] F. J. Wegner, J. Phys. C **7**, 2109 (1974).
[31] D. J. Bergman and B. I. Halperin, Phys. Rev. B **13**, 2145 (1975).
[32] M. Hagen, H. R. Child, J. A. Fernandez-Baca, and J. L. Zaretsky, J. Phys. Condens. Matter **4**, 8879 (1992).
[33] H. Lin, M. F. Collins, and T. M. Holden, J. Appl. Phys. **73**, 5341 (1993).